ELECTRICAL AND ELECTROCHEMICAL CHARACTERISTICS OF A NEW TYPE OF POLYACETYLENE FILMS

Jiří PFLEGER[a], Ivan KMÍNEK[a], Stanislav NEŠPŮREK[a],
Vítězslav PAPEŽ[b] and Petr NOVÁK[b]

[a] *Institute of Macromolecular Chemistry, Czechoslovak Academy of Sciences, 162 06 Prague 6 and*
[b] *The J. Heyrovský Institute of Physical Chemistry and Electrochemistry, Czechoslovak Academy of Sciences, 182 23 Prague 8*

Received July 6, 1988
Accepted September 2, 1988

The morphology, electrochemical and electrical properties of polyacetylene films, prepared with a catalytic system titanium tetrabutoxide/ethylmagnesium bromide in two forms — non-dried porous and dried compact ones — were studied. The properties of non-dried porous films as positive electrodes in lithium cells were characterized by means of cyclic voltammetry, electrochemical impedance measurements, galvanostatic cycling and "in situ" resistance measurements. The electrical conductivity of undoped dried compact films was 10^{-7} to 10^{-6} S m^{-1} depending on the oxygen content. Iodine doping increased the conductivity of these films up to $\sigma = 7{\cdot}6 \cdot 10^3$ S m^{-1}, the conductivity of the *trans*-isomer $(CHI_{0.27})_x$ increased up to $\sigma = 3{\cdot}3 \cdot 10^3$ S m^{-1}. From the temperature dependence of the electrical conductivity we have concluded that the transport of charge carriers is due presumably to the variable-range, phonon-assisted hopping of carriers between localized states, the density distribution function of which is not constant around the Fermi level.

A considerable amount of research has been done on different organic electroactive polymers as electrodes in advanced secondary batteries, e.g., on polypyrrole[1], polythiophene[2], and other electrochemically generated polymers[3], but polyacetylene, $(CH)_x$, has been so far the most often studied polymeric active electrode material for lithium cells[4-7]. Utilization of all the above-mentioned electroactive polymers in electrochemical cells is based on a reversible insertion of anions or sometimes cations into the polymer structure, often called the doping/undoping process. Polyacetylene can be doped by chemical or electrochemical methods using different ions and solvents, but the most usual procedure for battery experiments is the electrochemical *p*-doping by ClO_4^- ions from aprotic solvents such as propylene carbonate. The doping/undoping process (i.e. charging/discharging) is connected with the diffusion and migration of ions in the bulk[5] of $(CH)_x$. In secondary polyacetylene batteries the best coulombic capacities reported for Shirakawa-type[8] $(CH)_x$ and for the "foam" polyacetylene[7,9] were about 340 Ah kg^{-1}. On the other hand, electrophore-

tically-deposited polyacetylene was found to be electrochemically inactive[10], probably because of irreversible doping.

The polymerization of acetylene has been carried out by using a number of catalysts[11]. At present, the catalytic system titanium tetrabutoxide/triethylaluminium is used almost exclusively, because $(CH)_x$ films thus obtained possess good electrical and electrochemical properties and good mechanical behaviour. Titanium in its alkoxides is reduced to effective catalysts of the Ziegler–Natta type also by many compounds containing metals of groups I – III other than alkyl derivatives of aluminium. It was found that the reaction products of titanium tetrabutoxide $Ti(OBu)_4$ with ethylmagnesium bromide (EtMgBr) are effective catalysts of acetylene polymerization[12]. Under the specific conditions a free-standing porous film with a bulk density of 70 to 100 kg m^{-3} was formed, containing about 90% of solvent. After extraction of the catalyst and drying a compact film of bulk density of about 900 to 1 050 kg m^{-3} was obtained[12].

We were interested in the evaluation of electrochemical activity of such polyacetylene films. The electrical properties of high density dried compact films were also studied.

EXPERIMENTAL

Material

A solution of $Ti(OBu)_4$ in diethyl ether (1 : 10 by vol.) was introduced at room temperature into a flat-bottom reactor and a diethyl ether solution of EtMgBr (1·4 mol/l) was added under stirring in such an amount that [Mg]/[Ti] = 2·5. The thickness of the liquid layer was c. 5 to 10 mm. After 10 min the catalytic solution was cooled without stirring to 195 K. After another 20 min pure dry acetylene was introduced above the surface and a $(CH)_x$ film was formed. The polymerization was stopped after 1 h by pouring an excess of a deaerated mixture of methanol and acetic acid (10 : 1 by vol.) into the cooled reactor. The mixture was then slowly heated to room temperature. The $(CH)_x$ film was separated from the bottom and extracted for 24 h several times with the same mixture as that used for termination. It was observed that drying of the film after extraction of the catalyst led to an anisotropic decrease in volume; the thickness dropped to 20 to 25% of the original value, the other dimensions decreased to c. 55 to 65%. At first sight, the samples had an apparent asymmetry: the surface facing the bottom of the reaction vessel was shiny, with golden-green lustre, while the other side was dull. This difference was also detected in scanning electron micrographs (see Fig. 1, *a*, *b*). The films seemed to be homogeneous in the bulk and no fibrillar structure (Fig. 1*c*) was detected at this resolution (magnification 10 000). If the films were mechanically fixed in a frame to prevent scratching during drying, in the dry state they had a 10 to 15% degree of orientation along the axis lying in the plane of the film, according to the wide-angle X-ray diffraction data (Fig. 2). In further measurements two types of samples were used: films stored and measured in propylene carbonate ("nondried porous films") with bulk density of about 100 kg m^{-3}, and films dried in vacuo in a frame ("dried compact films") having the density of about 900 – 1 050 kg m^{-3} and the specific surface area of 0·3 – 0·4 m^2 g^{-1}.

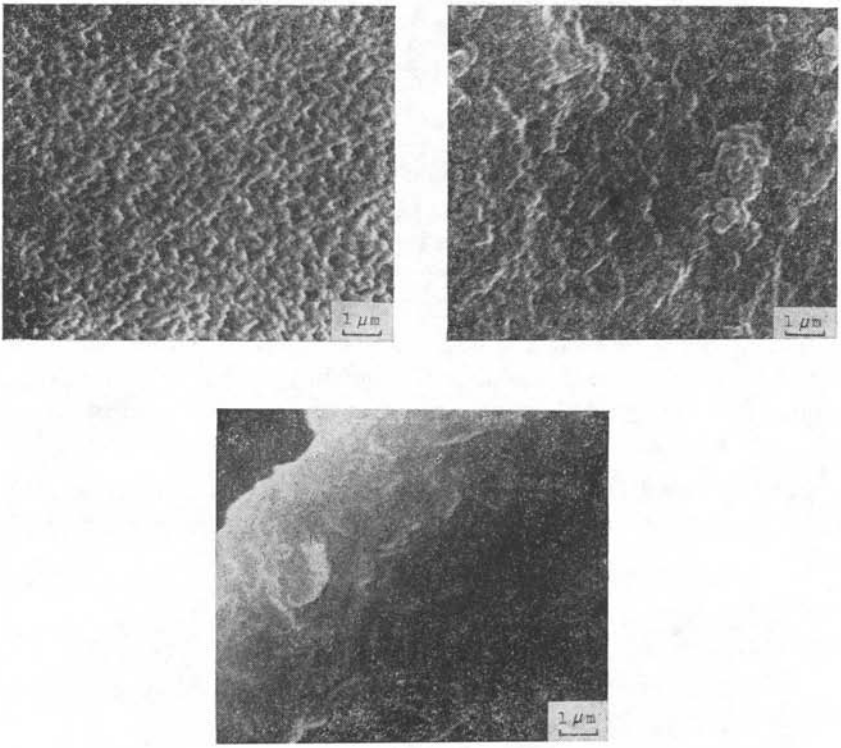

FIG. 1

Scanning electron micrographs of the dried compact polyacetylene film: *a* Shiny surface, *b* dull surface, *c* cross-section of the glass-substrate (shiny) part of the sample

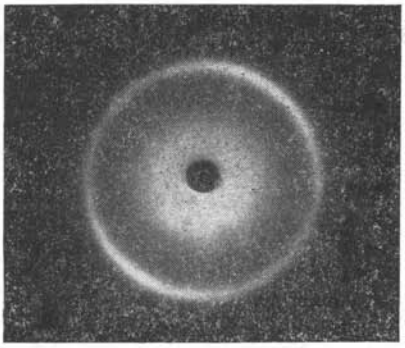

FIG. 2

Wide angle X-ray diffraction pattern of the dried compact polyacetylene film

It was found from the integral intensities of scattered radiation in wide-angle X-ray scattering (WAXS) measurements that the degree of crystallinity of non-isomerized dried films exceeded 70%, i.e., the crystallinity of this material was similar to that of Shirakawa films[11]. The diameter of the crystallites was estimated as 6 nm.

As shown by IR spectra (Fig. 3), the dried compact films contained about 40% *trans*-$(CH)_x$. During 2 h isomerization at 410 K and a pressure of 10^{-3} Pa the content of *trans*-$(CH)_x$ increased to 90%, as determined from the peak intensities[8] at 740 cm^{-1} (*cis*-form) and 1 015 cm^{-1} (*trans*-form) (see Fig. 4). These samples contained $3 . 10^{19}$ spins per cm^3 according to ESR.

Dry as-grown (non-isomerized) $(CH)_x$ films possessed good mechanical properties. Their initial modulus in the elastic region was comparatively high (≈900 MPa). The yield point was distinctly indicated and at $l/l_0 \geqq 1{\cdot}1$ plastic flow and cold drawing set in. Although the polymer contained a considerable amount of the *trans*-isomer, narrow 2 mm strips could be drawn up to $l/l_0 \approx 3{\cdot}8$, even at high rates of deformation ($>1{\cdot}0\ s^{-1}$). Fig. 5 shows the stress-strain dependence. As expected, thermally isomerized *trans*-films could not be drawn, but they were very flexible.

Iodine-doped dried compact films were prepared by exposure in iodine vapour (40 Pa, 298 K, nitrogen atmosphere). The doping level was controlled by weighing.

Electrochemical Measurements

All electrochemical measurements were performed at room temperature with a Li counter-electrode and 1M-$LiClO_4$ in propylene carbonate electrolyte (water content less than 50 ppm) in a spring-loaded (0·1 MPa) stainless-steel two-electrode cell. We assumed throughout that the potential of the Li counter-electrode was stable within few tens of millivolts; we therefore refer all potentials to this Li counter-electrode (Li/Li^+ scale). The polyacetylene foil (1·77 cm^2) was placed between two electrically isolated stainless-steel gauzes (current collectors). Four layers of non-woven polypropylene BASEP 108 separator and two layers of a low-porosity filter paper were used to avoid short-circuiting caused by the formation of Li dendrites. An electrolyte reservoir (1 cm^3) was used to wet the separators.

The current collectors on both polyacetylene sides were short-circuited during all electrochemical measurements. For the "in situ" resistance measurements the current collectors were disconnected and a small potential difference (some tens of millivolts) was applied across both current collectors for a short time with another potentiostat. The current flowing through the polyacetylene electrode was measured with a nanoampermeter and the resistance of the electrode was then calculated.

All cells were prepared in an argon-filled glove box to avoid contamination with oxygen or water. After assembling, the cells were vacuum-degassed and sealed hermetically. Cyclic voltammetric measurements were done with a potentiostat PS4 and a variator PV3 (both from Forschungsinstitut Meinsberg, G.D.R.). Galvanostatic cycling with data recording was performed with a SAPI 80 computer with an in-house built electrochemical interface. Electrochemical impedances were measured with a Solartron 1 250 Frequency Response Analyser with a Solartron 1 286 Electrochemical Interface in the frequency range 65 kHz — 100 μHz.

Electrical and Related Measurements

The electrical conductivity σ of dried compact films was measured by the standard d.c. four-probe method. Platinum contacts were applied mechanically to the samples. The temperature dependence of conductivity was measured on sandwich type samples with guard ring using vacuum deposited gold electrodes. The current was measured by a Keithley 616 electrometer with a Keith-

ley 247 power supply. IR spectra of 10 μm thick films were recorded with a Perkin–Elmer 580 B apparatus, the specific surface area was measured by the BET method using a Quantasorb apparatus, the stress-strain dependences were measured using an Instron apparatus after the film had been exposed to air for one hour at most. The morphology was tested with a JEOL JSM 35 scanning microscope, X-ray diffraction was recorded with an automatic diffractometer HZG 4A.

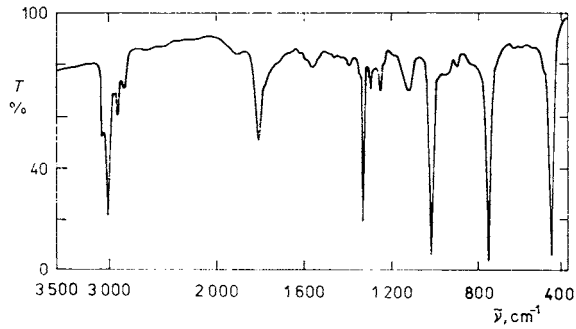

FIG. 3

IR spectrum of the as-grown dried compact polyacetylene film

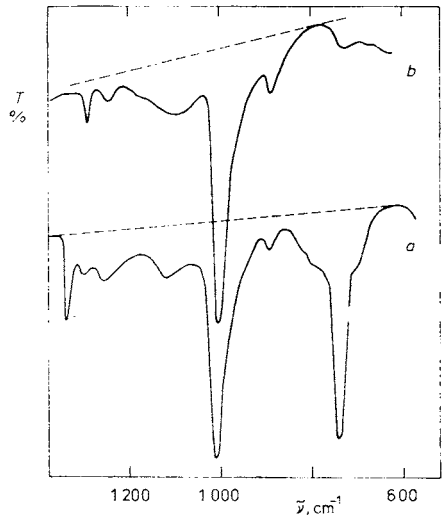

FIG. 4

IR spectra of the polyacetylene films. *a* As-grown dried compact film, *b* film isomerized at 410 K and 10^{-3} Pa

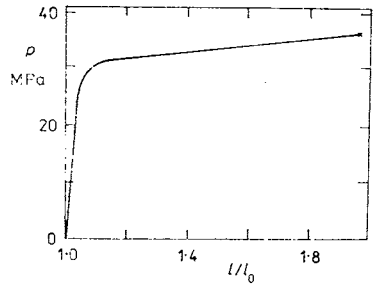

FIG. 5

Stress-strain dependence of the dried compact polyacetylene film (57% *cis*-structure); rate of deformation 0·8 min^{-1}

RESULTS AND DISCUSSION

Electrochemical Measurements

The electrochemical behaviour of non-dried "porous" polyacetylene was studied on films 140 and 400 μm thick. A typical repetitive cyclic voltammogram is shown in Fig. 6 and the corresponding charges for oxidation and reduction of the material during subsequent cycles are listed in Table I. A comparison of our Fig. 6 with the results from ref.[7] shows clearly that the shape and position of the peaks of our $(CH)_x$ are generally similar to those of Scrosati's[7] "foam" $(CH)_x$, but the oxidation and reduction peak separation is slightly larger for our material (about 400 mV). The main reason is that we measured relatively thick dense films with very low porosity in contrast to the "foam" type material[7]. From the morphological point of view we therefore expected the insertion of ClO_4^- anions into $(CH)_x$ to be more hindered. The rate-determining step in the doping process was the diffusion of ClO_4^- anions in the bulk of the electrode as shown clearly by the dominating Warburg impedance in the complex impedance diagram (Fig. 7).

The comparison of the shape of the cyclic voltammograms for different sweep rates is interesting. During fast sweeps (10 mV s^{-1}) the polyacetylene is gradually "activated" – the total charge for oxidation and reduction slightly increases with

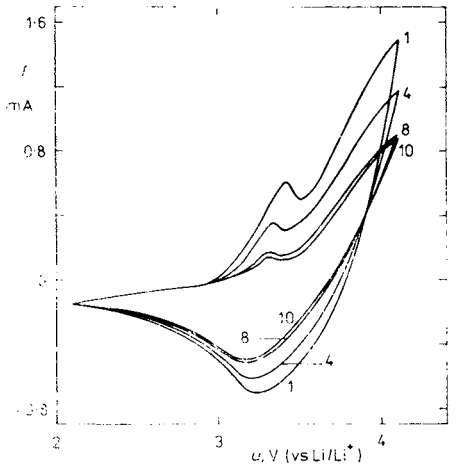

FIG. 6

Repetitive cyclic voltammogram of a porous, 400 μm thick polyacetylene film at 0·17 mV . . s^{-1}. Cycle numbers are denoted in the figure

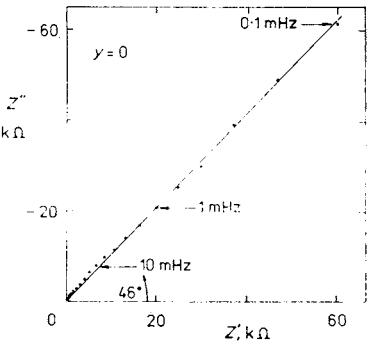

FIG. 7

Typical impedance diagram of virgin 140 μm thick film of porous polyacetylene

the cycle number (see Fig. 8). We believe that during subsequent cycles the doped (and therefore electronically conducting) surface layer gradually grows into the bulk of virgin and non-conducting polyacetylene. The increasing conductivity in the bulk of the electrode leads to a better utilization of the material. On the other hand, during slow sweeps (0·17 mV s^{-1}, Fig. 6) there is enough time to dope the bulk of the electrode during the first cycle. In this case the total coulombic capacity decreases with the cycle number (Table I) because the doping level is rather high (about 2 mole %) and some charges are probably blocked by the equivalent amount of anions irreversibly bonded[2] in the bulk of $(CH)_x$.

The doping process was further studied by the "in situ" resistance measurements of polyacetylene films during cycling. Cathode resistances (measured after potentio-

TABLE I

Oxidation (Q_{charge}) and reduction (Q_{disch}) charges and doping levels y from repetitive cyclic voltammograms at 0·17 mV s^{-1} for 400 μm thick "porous" polyacetylene films

Cycle No.	Q_{charge} C	Q_{disch} C	Q_{disch}/Q_{charge}	y mole %
1	6·0	4·2	0·70	2·7
2	4·8	3·9	0·81	2·2
3	4·2	3·8	0·91	1·9
4	4·6	4·0	0·87	2·0
6	3·7	3·3	0·89	1·7
10	3·3	2·9	0·88	1·5

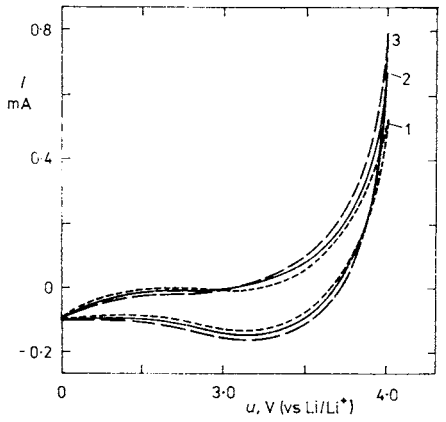

FIG. 8

Repetitive cyclic voltammogram of porous, 140 μm thick polyacetylene film at 10·1 mV . . s^{-1}. Cycle numbers are denoted in the figure

static steps when the current fell down to 10 μA) are summarized in Table II, as a function of the cycle number and the potential of the electrode. In conformity with the well-known behaviour of polyacetylene, the resistance of the electrode decreased by several orders of magnitude during oxidation (doping), but when the oxidized electrode was reduced back to the neutral state the resistance did not increase to the original level. Assuming that the electronic conductivity of $(CH)_x$ depends on the doping level (i.e. on the concentration of anions bonded by the coulombic interactions in the $(CH)_x$ structure), our results confirm that a part of the stored charge is more or less irreversibly bound in the electrode. The amount of this charge naturally depends on the current selected as zero value (10 μA in our case) for the termination of charging or discharging. If this current is lowered, the residual charge bonded in the electrode becomes also lower, and the resistance of polyacetylene increases, but within a finite time it never reaches the very high value of the virgin material.

The polyaceylene films were further cycled galvanostatically with the Li counter-electrode. The typical result is shown in Fig. 9. The cell was charged for 1·5 h with 200 μA (this charge corresponds to the doping level $y = 0{\cdot}5$ mole %) and discharged for 1·5 h with 125 μA. Thus the coulombic efficiency could be estimated as 62·5% and the doping level as 0·5 mole %. In this regime the final $(CH)_x$ potential after the complete charge/discharge cycle increased from 1·7 to 3·25 V during the first 8 cycles. During further cycling the final potential was found to be nearly constant. Since the coulombic efficiency was only 62·5% during each cycle, the charge equivalent to the doping level of 0·18 mole % was left in the bulk of the electrode. The irreversible doping level of 1·5 mole % was thus reached after 8 cycles. Both the shape and position of the charge/discharge curves were thereafter rather independent of the cycle number (Fig. 9). From these galvanostatic results (which are in good agreement with the cyclic voltammetric data on the same $(CH)_x$, we assume that during

TABLE II

The "in situ" resistance of the potentiostatically charged and discharged polyacetylene films

Cycle No.	Electrode potential V vs Li/Li^+	Resistance kΩ
1-Virgin A	open circuit	1 000
1-Charged	3·40	30
2-Discharged	2·40	43
2-Charged	3·40	7·3
3-Discharged	2·40	57
3-Charged	3·40	8·6
4-Discharged	2·40	43

the first 8 cycles the bulk of the polyacetylene electrode is doped (and therefore electrochemically "activated") enough to allow a steady-state cycling. Hence, we have inferred from our own resistance measurements and also from the data of ref.[13] that the most important rise in the conductivity of polyacetylene lies below the doping level of 1 mole %. Thus, both methods showed that the nearly steady-state electrochemical behaviour was reached when the average doping level was 1 to 1·5 mole %.

All our measurements explained the necessity to perform several preliminary cycles before polyacetylene reached the steady-state behaviour during various types

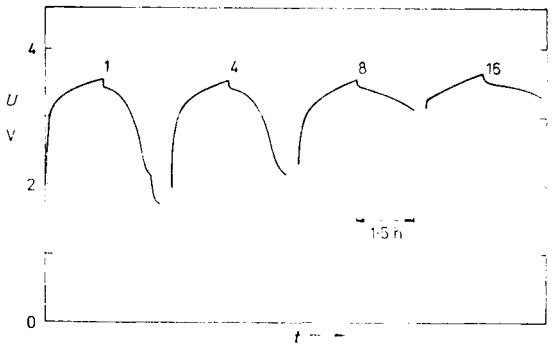

FIG. 9

Typical charge (I_{ch} = 250 μA) and discharge (I_{disch} = 125 μA) curves for porous, 400 μm thick polyacetylene film (weight 29 mg). Number of cycles is indicated

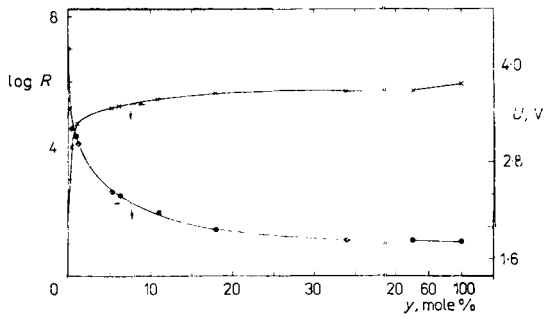

FIG. 10

Dependence of the "in situ" resistance R of a 140 μm thick, porous polyacetylene electrode and of the voltage U of the Li(CH)$_x$ cell as a function of the doping level y. Galvanostatic charging with 15 μA cm^{-2}

of cycling (the number of cycles depends on the rate of formation of the electronically conducting material) from the originally rather insulating one.We believe that this process is completed after a few cycles; another question therefore arises, viz. what is the reason for the rather high self-discharge rate observed during further cycling, i.e., why the coulombic efficiency during galvanostatic cycling is only 62%.

In an attempt to contribute to the solution of the self-discharge problem, we measured the dependence of the "in situ" resistance of the cathode and of the voltage of the $Li/(CH)_x$ cell during uninterrupted galvanostatical charging at very low current densities (around 15 $\mu A\ cm^{-2}$) on the doping level y. From Fig. 10 it is clear that at the beginning of charging the resistance decreases very rapidly with the doping level y from 10^7 to $10^2 - 10^1\ \Omega$. Upon further charging (oxidation, $y > 20$ mole %) the decrease in the resistance is only very small until $y = 100$ mole % (i.e. one ClO_4^- per one CH unit) is reached; at this point the experiment was interrupted. Nearly the same type of behaviour was observed for the voltage-doping level relationship, where the voltage never exceeded 3·8 V.

We deduce from these experiments that the oxidation (doping) of polyacetylene reaches about 15–20 mole %, whereas the cell voltage approaches the maximal value of 3·8 V (for the low current density of 15 $\mu A\ cm^{-2}$). Further galvanostatic charging does not raise the voltage or the cathode conductivity. As follows from Fig. 10, further overcharging of the cell does not degrade polyacetylene (at least from the point of view of the electronic conductivity) and probably does not raise the real doping level, because in the opposite case further doping (oxidation) up to one ClO_4^- per one CH unit would probably irreversibly degrade the $(CH)_x$ structure and decrease its electronic conductivity. We expect that as the limiting voltage of the cell is approached, steady-state is reached (depending on the current density, which must be low enough) and the charging rate becomes equal to the self-discharge rate. This phenomenon seems to be very important as it leads to an instrinsic protection of real cells against galvanostatic overcharge.

In order to develop our hypothesis further, it is necessary to disclose the nature of the current-consuming parasitic (self-discharge) reaction. One possible explanation is that the electrolyte (1M-$LiClO_4$ in propylene carbonate) decomposes at a potential of about 3·8 V (Li/Li^+), i.e. about 500 mV below the decomposition potential observed at the bare stainless-steel current collector. The question, however, remains whether the effect is due to the catalytic activity of polyacetylene or whether the reason lies merely in a very large difference in the active surface areas of both electrodes. Some attempts to elucidate these problems will be the subject of further work.

Electrical Properties

The dark d.c. conductivity of undoped dried compact *trans*-form of $(CH)_x$ at room temperature in the vacuum 10^{-4} Pa was found to be $\sigma = 1{\cdot}2 \cdot 10^{-7}\ S\ m^{-1}$. The

temperature dependence of conductivity is plotted in Fig. 11 as $\log \sigma$ vs T^{-1}, $\log \sigma$ vs $\log T$, and $\log \sigma$ vs $T^{-1/4}$. The activation energy W_a in the medium temperature region (180 to 270 K) was determined from the first plot according to the relation $\sigma = \sigma_0 \exp(-W_a/kT)$ (where k is the Boltzmann constant and σ_0 is the pre-exponential factor) as 0·42 eV. W_a was 0·51 eV above 300 K. Over the temperature range investigated the temperature dependence of conductivity seems to obey the relation $\sigma \sim T^n$ (Kivelson's model[14]), where n is a constant. The best fit of experimental data in Fig. 11 was obtained with $n = 19$ (solid line 2).

Kivelson's model is based on an assumption that both a neutral S_0 and a charged soliton S_+ are present in $(CH)_x$, the former mobile, the latter localized by Coulomb attraction in the vicinity of charge impurity. The hopping probability between the sites is large enough below room temperature only in the case that S_0 is situated just near an impurity. The electrical conductivity is then given by a relation derived by Kivelson[14] on the basis of a general model for hopping transport developed by Miller and Abrahams[15]

$$\sigma = A \frac{e^2 \gamma(T)}{kTN} (\xi/R_0^2) \frac{y_n y_{ch}}{(y_n + y_{ch})^2} \exp(-2BR_0/\xi), \qquad (1)$$

where A, B are constants, y_n and y_{ch} are the concentrations of neutral and charged solitons per one carbon atom, respectively, $R_0 = [(4/3)\pi c_{imp}]^{-1/3}$ is a typical separation distance between impurities (of concentration c_{imp}), ξ is the dimensionally averaged decay length of the soliton, and N is the number of carbon atoms per $(CH)_x$ chain. The characteristic frequency $\gamma(T)/N$ is proportional to the probability that the energy difference between the states S_0 and S_+ does not exceed kT. The rate of the hopping transitions is averaged over the thermal distribution of initial and final site energies. Kivelson's theory gives the dependence $\gamma(T) = 2\pi h^{-1} \gamma_0 (T/T_0)^{n+1}$, where γ_0 and T_0 are constants.

According to experimental data (curve 2, Fig. 11), Kivelson's model seems to be a good representation of transport properties. However, the obtained value $n = 19$ is too high and contrasts with that obtained for the Shirakawa-type $(CH)_x$ where n varies[16,17] from 9 to 14 as well as with the value proposed by Kivelson[14] ($n \approx 10$).

A third possibility was therefore tested: the conductivity data were analyzed in terms of variable range, phonon-assisted hopping between localized states (the $\log \sigma$ vs $T^{-1/4}$ dependence). In the simplest case of isotropic three-dimensional hopping among localized states with a constant energy density near the Fermi level E_F, the conductivity is determined by three parameters only: the density of states ϱ_F, characteristic frequency ν_0 (where ν_0 is proportional to temperature[15]), and the localization length ξ. Then we have for the d.c. conductivity[18]

$$\sigma_{d.c.} = \sigma_0' \exp[-(T_0/T)^{1/4}], \qquad (2)$$

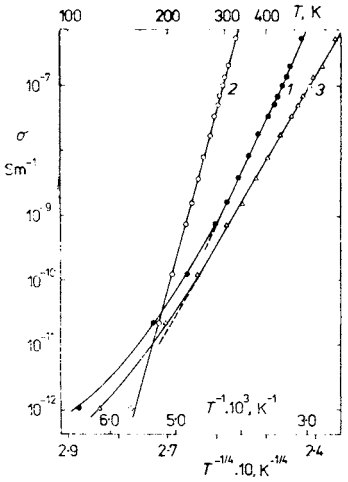

FIG. 11

Dependence of the electric conductivity σ on the temperature of the dried compact *trans*-polyacetylene film. *1* In the coordinates $\log \sigma$ vs T^{-1} (the dashed line represents the activation energy $W_a = 0{\cdot}42$ eV); *2* in the coordinates $\log \sigma$ vs $\log T$ (solid line represents the best fit for $n = 19$); *3* in the coordinates $\log \sigma$ vs $T^{-1/4}$ ($T_0 = 8 \cdot 10^9$ K)

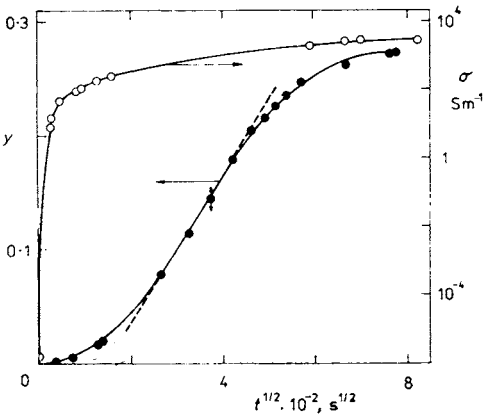

FIG. 12

Dependence of iodine concentration y and electric conductivity σ on the time t of treatment in iodine vapours

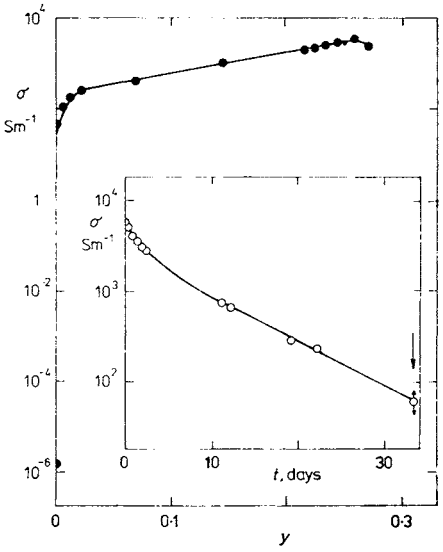

FIG. 13

Dependence of the electric conductivity σ on the iodine doping level y of the dried compact polyacetylene film. Inset: Dependence on the time of air exposure of the electric conductivity σ of a sample doped to maximal conductivity

where $T_0 = 75/(\xi^3 \pi k \varrho_F)$, $\sigma'_0 = 1{\cdot}34e^2 \nu_0/kT$. Thus, in the range of validity of this theory (i.e. for $(T_0/T)^{1/4} \geqq 7{\cdot}5$), σ_{dc} follows the well-known Mott's $T^{-1/4}$ law. The value $T_0 = 8 \cdot 10^9$ K was obtained from experimental data (Fig. 11, curve *3*, temperature interval from 210 to 320 K). The density of states estimated from T_0 gives $8 \cdot 10^{23}$ m^{-3} eV^{-1}, under the assumption that the localization length is $3{\cdot}56 \cdot 10^{-10}$ m. The deviation of experimental points from the log σ vs $T^{-1/4}$ line in the low temperature region ($T < 210$ K) could be explained by a non-constant distribution function of localized states density around the Fermi level[16], as considered in the model of Summerfield and Chroboczek for intersoliton hopping. This assumption is in agreement with our preliminary results of a.c. conductivity measurements.

The electrical conductivity of dried compact *trans*-$(CH)_x$ increased by 9 orders of magnitude in iodine-doped samples (treated in nitrogen atmosphere by iodine vapour at a pressure of about 40 Pa, temperature 298 K). The time dependence of the doping level and conductivity during the doping procedure is given in Fig. 12. The dependence of conductivity on the iodine content (obtained by weighing) is given in Fig. 13. The maximum conductivity value was obtained at the doping level $y \approx 0{\cdot}27$ mole % and reached $3 \cdot 10^3$ to $5 \cdot 10^3$ S m^{-1} in various samples. The stability of such conducting films in an open atmosphere was not good. As follows from the inset of Fig. 13, during 10 days the conductivity value decreased by an order of magnitude and for longer times a slower further decrease was detected.

CONCLUSION

The electric conductivity of undoped dried compact polyacetylene films prepared with the catalytic system titanium tetrabutoxide/ethylmagnesium bromide was 10^{-7} to 10^{-6} S m^{-1}, depending on the oxygen content. The transport of charge carriers was due presumably to the variable range, phonon-assisted hopping of carriers between localized states. Iodine doping increased the conductivity of these films up to $\sigma = 5 \cdot 10^3$ S m^{-1}. The electrochemical activity of non-dried porous films was conditioned by oxidation to the level of $y \approx 1$ mole %. This oxidation charge was bound very firmly so that it cannot be used in discharging the PA electrode. The cell Li|1M-$LiClO_4$, propylene carbonate |PA was subject to self-discharge already at a voltage of 3·6–3·7 V, hence no deterioration of the PA electrode takes place during overcharging the cell with low constant currents (10–20 μA cm^{-2}). The maximum coulombic capacity 39 Ah kg^{-1} was reached at the expense of the stability of the electrode.

REFERENCES

1. Mohammadi A., Inganäs O., Lundström I.: J. Electrochem. Soc. *133*, 947 (1986).
2. Scrosati B., Panero S., Prosperi P., Corradini A., Mastragostino M.: J. Power Sources *19*, 27 (1987).

3. Diaz A. F., Bargon J.: *Handbook of Conducting Polymers* (T. A. Skotheim, Ed.), p. 81. Marcel Dekker, New York 1986.
4. Nagamoto T., Ichikawa C., Omoto O.: J. Electrochem. Soc. *134*, 305 (1987).
5. Armand M.: J. Phys. *44*, C3-551 (1983).
6. Passiniemi P., Österholm J. E.: Mol. Cryst. Liq. Cryst. *121*, 215 (1985).
7. Padula A., Scrosati B.: J. Power Sources *14*, 31 (1985).
8. Ito T., Shirakawa H., Ikeda S.: J. Polym. Sci. *12*, 11 (1974).
9. Shacklette L. W., Toth J. E., Murthy N. S., Baughman R. J.: *Extended Abstracts, Meeting of the Electrochem. Society, New Orleans, October 7—12, 1984*; Abst. No. 619, p. 900.
10. Papež V., Novák P., Pfleger J., Kmínek I., Nešpůrek S.: Electrochim. Acta *32*, 1087 (1987).
11. Saxman A. M., Liepins R., Aldissi M.: Prog. Polym. Sci. *11*, 57 (1985).
12. Kmínek I., Trekoval J.: Makromol. Chem., Rapid. Commun. *7*, 53 (1986).
13. Shacklette L. W., Chance R. R., Elsenbaumer R. L., Baughman R. H.: *Proc. 30th Power Sources Symp., Atlantic City June 7—10, 1982*, p. 66.
14. Kivelson S.: Phys. Rev., B *25*, 3798 (1982).
15. Miller E., Abrahams E.: Phys. Rev. *120*, 745 (1960).
16. Summerfield S., Chroboczek J. A.: Solid State Commun. *53*, 129 (1985).
17. Epstein A. J., Rommelman H., Abkowitz M., Gibson H. W.: Phys. Rev. Lett. *47*, 1549 (1981).
18. Ehinger K., Roth S.: Phil. Mag., B *53*, 301 (1986).

Translated by L. Kopecká.